AIAA-98-4261

In-Flight System Identification

Eugene A. Morelli

NASA Langley Research Center
Hampton, VA

AIAA Atmospheric Flight Mechanics Conference
August 10 - 12, 1998 / Boston, MA

AIAA-98-4261

IN-FLIGHT SYSTEM IDENTIFICATION

Eugene A. Morelli

Research Engineer
NASA Langley Research Center
Hampton, Virginia USA 23681 - 2199

Abstract

A method is proposed and studied whereby the system identification cycle consisting of experiment design and data analysis can be repeatedly implemented aboard a test aircraft in real time. This adaptive in-flight system identification scheme has many advantages, including increased flight test efficiency, adaptability to dynamic characteristics that are imperfectly known *a priori*, in-flight improvement of data quality through iterative input design, and immediate feedback of the quality of flight test results. The technique uses equation error in the frequency domain with a recursive Fourier transform for the real time data analysis, and simple design methods employing square wave input forms to design the test inputs in flight. Simulation examples are used to demonstrate that the technique produces increasingly accurate model parameter estimates resulting from sequentially designed and implemented flight test maneuvers. The method has reasonable computational requirements, and could be implemented aboard an aircraft in real time.

Nomenclature

a_x, a_y, a_z	body axis translational accelerations, g
$E\{\cdot\}$	expectation operator
$\boldsymbol{A}, \boldsymbol{B}, \boldsymbol{C}, \boldsymbol{D}$	linear system matrices
g	acceleration due to gravity, ft/sec^2
h	altitude, ft
J	cost function
L	aerodynamic lift force
M	Mach number
N	total number of sample times
p, q, r	body axes angular velocities, rad/sec
Re	real part
$\boldsymbol{R}$	measurement noise covariance matrix
Tr	trace
$\boldsymbol{u}$	control vector
V	airspeed, ft/sec
$\boldsymbol{x}$	state vector
$\boldsymbol{y}_i$	output vector at time $i\Delta t$
$\boldsymbol{z}_i$	measured output vector at time $i\Delta t$
Z	z body axis aerodynamic force
$\boldsymbol{0}$	zero vector
α	angle of attack, rad
δ_{ij}	Kronecker delta
Δt	sampling interval, sec
ω	angular frequency, rad/sec
θ	p-dimensional parameter vector

superscripts

T	transpose
*	complex conjugate transpose
$\tilde{}$	discrete Fourier transform
$\hat{}$	estimate
-1	matrix inverse

subscripts

o	trim or initial value
w	wind axes

Introduction

Flight testing to collect data for dynamic modeling begins with some *a priori* information about the aircraft dynamics. The *a priori* information typically consists of the rigid body equations of motion in conjunction with aerodynamic and engine data from ground tests. Flight test maneuvers are designed to excite the dynamic response of the aircraft, based on

the *a priori* information to produce data for dynamic modeling. The maneuvers are then scheduled for flight test, executed by either the pilot or an on-board computer system in flight, and the data is recorded for post-flight analysis. Because of differences between flight test results and predictions based on ground tests, the maneuver design based on *a priori* information may turn out to be deficient in some way. For example, if the input amplitude is too low, the data will have low information content, which leads to inaccurate model parameter estimates. A similar data information deficiency can result if the input frequencies are poorly chosen. On the other hand, if the input amplitude is too high, the aircraft motion may stray too far from the test condition or excite nonlinearities, which can invalidate modeling assumptions made for both the maneuver design and the data analysis. Typically, these problems are discovered during post-flight data analysis, resulting in a need for additional flight tests. Such additional experimentation requires more flight time, more engineering time, and more money, which are seldom readily available. A block diagram of the entire process appears as Figure 1.

One iteration through the identification cycle shown in Figure 1 can easily take months or even years in practice. The main difficulty is the large time delay that occurs due to the analysis and scheduling of additional maneuvers, and the inevitable conflict of the requirement for more flight time to collect dynamic modeling data with other objectives of the flight test program.

This work examines a different approach to obtaining the requisite data for dynamic modeling purposes. Figure 2 illustrates the idea. Analysis is now done in real time aboard the aircraft, so that modeling results from an initial maneuver could be used to design the subsequent test maneuver, and so on throughout the flight test until acceptable results (e.g., specific model parameter accuracies) are achieved. The result is an adaptive experiment design and data analysis method that is carried out in flight. With this approach, the quality of modeling results based on the measured flight data would be known before the aircraft lands, and no further flights would be required for this purpose. At the very least, the procedure could provide a high level of confidence that sufficient high quality data was collected for the modeling task, and could do so in one flight. Flight testing in this way would therefore greatly increase efficiency and effectiveness, since the complete identification cycle would be carried out in flight in an automated fashion. In addition, detailed *a priori* information would not be required to design the maneuver in this case, since the maneuver design starts by using a very simple low amplitude input, and then evolves the input to more complex forms with appropriate amplitudes based on analysis of data from the preceding maneuvers.

There are many candidate methods for the in-flight data analysis and maneuver design, but the main requirement that they be simple enough to be implemented in real time aboard the aircraft narrows the field. In particular, any methods that iterate through the recorded data must be eliminated. One possibility is to use an extended Kalman filter to estimate the model parameters. This approach has been described in the literature[1], along with several specific applications to aircraft parameter estimation problems[2-5]. There are some problems with this approach, however, some of which are related to the fact that the constant model parameters are treated as additional states, which can therefore vary with time. In addition, numerical and convergence problems related to the requisite linearization and noise variance estimation can be encountered.

In this work, a simple recursive computation of the Fourier transform is used to implement equation error in the frequency domain for in-flight model parameter estimation. The in-flight maneuver design is done by creating simple square wave input forms with progressively increasing complexity, based on the latest results from the in-flight model parameter estimation. Together, these techniques adaptively carry out the complete system identification cycle in flight, using simple methods that can be implemented on modern flight computers.

The next section gives the problem statement and outlines the necessary theory. Following this, the in-flight system identification method is applied to a simulation example, where a linear truth model is used with outputs corrupted by noise similar to that observed in flight. The application is identifying an accurate model for the rigid body short period dynamics of a conventional fighter. Finally, a nonlinear simulation is used to demonstrate the in-flight system identification procedure.

Theoretical Development

Airplane dynamics can be described by the following linear model equations:

$$\dot{\boldsymbol{x}}(t) = \boldsymbol{A}\boldsymbol{x}(t) + \boldsymbol{B}\boldsymbol{u}(t) \tag{1}$$

$$\boldsymbol{x}(0) = \boldsymbol{x}_o \tag{2}$$

$$\boldsymbol{y}(t) = \boldsymbol{C}\boldsymbol{x}(t) + \boldsymbol{D}\boldsymbol{u}(t) \tag{3}$$

$$z_i = y_i + v_i \qquad i = 1, 2, \ldots, N \tag{4}$$

The discrete measurement noise vector v_i is assumed Gaussian with

$$E\{v_i\} = \boldsymbol{0} \quad \text{and} \quad E\{v_i\, v_j{}^T\} = \boldsymbol{R}\,\delta_{ij} \tag{5}$$

Matrices $\boldsymbol{A}$, $\boldsymbol{B}$, $\boldsymbol{C}$, and $\boldsymbol{D}$ in Eqs. (1) and (3) contain stability and control derivatives, which are the constant model parameters to be estimated from flight test data. The input quantities are control surface deflections, with output quantities from air data (V, α, β), body axis angular velocities (p, q, r), Euler angles (ϕ, θ, ψ), and translational accelerations (a_x, a_y, a_z). Longitudinal and lateral cases can be treated separately, with the linear model structure shown above resulting from the usual small perturbation assumptions[6].

The linear model structure given here will be used for the in-flight maneuver design and the in-flight data analysis. Using the linear model structure keeps the in-flight calculations simple, and is adequate for the purpose at hand, which is to adaptively design flight test maneuvers that produce good flight test data. If necessary, more sophisticated modeling and data analysis techniques can be applied to the measured data post-flight.

Equation Error in the Frequency Domain

The finite Fourier transform of a signal $x(t)$ is defined by

$$\tilde{x}(\omega) \equiv \int_0^T x(t) e^{-j\omega t} dt \tag{6}$$

which can be approximated by

$$\tilde{x}(\omega) \approx \Delta t \sum_{i=0}^{N-1} x_i\, e^{-j\omega t_i} \tag{7}$$

Subscript i indicates the variable value at time $i\,\Delta t$, and Δt is the sampling interval. The summation in Eq. (7) is defined as the discrete Fourier transform,

$$X(\omega) \equiv \sum_{i=0}^{N-1} x_i\, e^{-j\omega t_i} \tag{8}$$

so that

$$\tilde{x}(\omega) \approx X(\omega)\Delta t \tag{9}$$

Some fairly straightforward corrections[7] can be made to Eq. (9) to remove the inaccuracy resulting from the fact that Eq. (9) is a simple Euler approximation to the finite Fourier transform of Eq. (6). If the sampling rate is much higher than the frequencies of interest (ω), then the corrections are small and can be safely ignored.

Applying the Fourier transform to Eqs. (1) and (3) gives

$$j\omega\tilde{\boldsymbol{x}}(\omega) = \boldsymbol{A}\tilde{\boldsymbol{x}}(\omega) + \boldsymbol{B}\tilde{\boldsymbol{u}}(\omega) \tag{10}$$

$$\tilde{\boldsymbol{y}}(\omega) = \boldsymbol{C}\tilde{\boldsymbol{x}}(\omega) + \boldsymbol{D}\tilde{\boldsymbol{u}}(\omega) \tag{11}$$

When the states, outputs, and inputs are measured, individual state or output equations from vector Eqs. (10) or (11) can be used in an equation error formulation to estimate the stability and control derivatives contained in matrices $\boldsymbol{A}$, $\boldsymbol{B}$, $\boldsymbol{C}$, and $\boldsymbol{D}$. For the kth state equation of vector Eq. (10), the cost function is

$$J_k = \frac{1}{2}\sum_{n=1}^{m} \left| j\omega_n\, \tilde{x}_k(\omega_n) - \boldsymbol{A}_k\, \tilde{\boldsymbol{x}}(\omega_n) - \boldsymbol{B}_k\, \tilde{\boldsymbol{u}}(\omega_n) \right|^2 \tag{12}$$

where $\boldsymbol{A}_k$ and $\boldsymbol{B}_k$ are the kth rows of matrices $\boldsymbol{A}$ and $\boldsymbol{B}$, respectively, and $\tilde{x}_k(\omega_n)$ is the kth element of vector $\tilde{\boldsymbol{x}}(\omega_n)$. There are m terms in the summation, corresponding to m frequencies of interest, and each transformed variable depends on frequency. Similar

cost expressions can be written for individual output equations from vector Eq. (11). Denoting the vector of unknown model parameters in $\boldsymbol{A}_k$ and $\boldsymbol{B}_k$ by θ, the problem can be formulated as a standard least squares regression problem with complex data,

$$\boldsymbol{Y}_c = \boldsymbol{X}_c\,\theta + \varepsilon_c \tag{13}$$

where

$$\boldsymbol{Y}_c \equiv \begin{bmatrix} j\omega_1\,\tilde{x}_k(\omega_1) \\ j\omega_2\tilde{x}_k(\omega_2) \\ \vdots \\ j\omega_m\tilde{x}_k(\omega_m) \end{bmatrix} \tag{14}$$

$$\boldsymbol{X}_c \equiv \begin{bmatrix} \tilde{\boldsymbol{x}}^T(\omega_1) & \tilde{\boldsymbol{u}}^T(\omega_1) \\ \tilde{\boldsymbol{x}}^T(\omega_2) & \tilde{\boldsymbol{u}}^T(\omega_2) \\ \vdots & \vdots \\ \tilde{\boldsymbol{x}}^T(\omega_m) & \tilde{\boldsymbol{u}}^T(\omega_m) \end{bmatrix} \tag{15}$$

and ε_c represents the equation error in the frequency domain. The least squares cost function is

$$J = \frac{1}{2}\left(\boldsymbol{Y}_c - \boldsymbol{X}_c\,\theta\right)^{\dagger}\left(\boldsymbol{Y}_c - \boldsymbol{X}_c\,\theta\right) \tag{16}$$

which is identical to the cost in Eq. (12). The parameter vector estimate that minimizes this cost function is computed from[8]

$$\hat{\theta} = \left[Re\left(\boldsymbol{X}_c{}^{\dagger}\boldsymbol{X}_c\right)\right]^{-1} Re\left(\boldsymbol{X}_c{}^{\dagger}\boldsymbol{Y}_c\right) \tag{17}$$

The estimated parameter covariance matrix is

$$cov\left(\hat{\theta}\right) \equiv E\left\{\left(\hat{\theta}-\theta\right)\left(\hat{\theta}-\theta\right)^T\right\} = \sigma^2\left[Re\left(\boldsymbol{X}_c{}^{\dagger}\boldsymbol{X}_c\right)\right]^{-1} \tag{18}$$

where the equation error variance σ^2 can be estimated from the residuals,

$$\hat{\sigma}^2 = \frac{1}{(m-p)}\left[\left(\boldsymbol{Y}_c - \boldsymbol{X}_c\,\hat{\theta}\right)^{\dagger}\left(\boldsymbol{Y}_c - \boldsymbol{X}_c\,\hat{\theta}\right)\right] \tag{19}$$

and p is the number of elements in parameter vector θ.

Recursive Fourier Transform

For a given frequency, the discrete Fourier transform in Eq. (8) at sample time i is related to the discrete Fourier transform at time $i-1$ by

$$X_i(\omega) = X_{i-1}(\omega) + x_i\,e^{-j\omega i\Delta t} \tag{20}$$

where

$$e^{-j\omega i\Delta t} = e^{-j\omega\Delta t}e^{-j\omega(i-1)\Delta t} \tag{21}$$

The quantity $e^{-j\omega\Delta t}$ is constant for a given frequency and constant sampling interval. It follows that the discrete Fourier transform can be computed for a given frequency at each time step using one addition in Eq. (20) and two multiplications – one in Eq. (21) using the stored constant $e^{-j\omega\Delta t}$ for frequency ω, and one in Eq. (20). There is no need to store the time domain data in memory when computing the discrete Fourier transform in this way, because each sampled data point is processed immediately. Time domain data from all preceding maneuvers can be used in each subsequent analysis by simply continuing the recursive calculation of the Fourier transform. More data from more maneuvers improves the quality of the data in the frequency domain without increasing memory requirements to store it. In addition, the Fourier transform is available at any time $i\,\Delta t$. The approximation to the finite Fourier transform is completed using Eq. (9).

Rigid body dynamics of piloted aircraft lie in the rather narrow frequency band of 0-1 Hz. It is therefore possible to select closely spaced fixed frequencies for the Fourier transform and the subsequent data analysis. In this work, frequency spacing of 0.02 Hz was found to be adequate, which gives 50 frequencies evenly distributed on the interval [0.02-1.0] Hz for each transformed time domain signal. Zero frequency is excluded to remove trim values and measurement biases. The number of time domain signals to be transformed is usually low (7 or less – more if there are many control surfaces), so that this approach requires a small amount of computer memory that is independent of the time length of the flight test maneuvers.

Test Maneuver Design

The specification of the flight test maneuvers (equivalently, the flight test inputs) has a major impact on the quality of the measured data for modeling purposes. The goal is to design an experiment which produces data from which model parameters can be accurately estimated. This translates into exciting the dynamic response modes such that the sensitivities of the model outputs to the parameters are high and correlations among the parameters are low. Designing an experiment which meets these objectives requires rich excitation of the system, which is frequently at odds with various practical constraints, such as the requirement that output amplitude excursions stay within specified limits in order to assure the validity of an assumed model structure.

Previous work[9,10] has shown that inputs optimized for parameter estimation experiments can be effectively designed using the $\mathcal{D}$-optimality criterion, wherein the input design cost J_I equals the sum of squares of estimated parameter variances:

$$J_I = Tr\left[E\left\{ \left(\hat{\theta} - \theta\right)\left(\hat{\theta} - \theta\right)^T \right\} \right] \qquad (22)$$

The analytical connection between the input time history and the achievable accuracy for the model parameter estimates based on the measured data is detailed in Ref. [9]. For the present purposes, it suffices to say that the connection is strong, which means that the input time history has a significant impact on the accuracy of the parameter estimates computed from measured data. The choice of input implicitly includes the length of the maneuver.

Doublet, 2-1-1, and 3-2-1-1 input forms have the advantages of easy implementation in flight and simple design based on current estimates of modal frequencies and steady state (dc) gain. Figures 3, 4, and 5 illustrate each input form.

Flight test results from Ref. [9] demonstrated that at low angle of attack, a simple 3-2-1-1 input form is roughly 25% less effective than a globally optimal square wave input which minimized the $\mathcal{D}$-optimality criterion given above.

The 3-2-1-1 has a very simple design procedure, which is:

1. Match the frequency of the 2 pulse to the current estimate of the natural frequency for the dominant oscillatory mode. Note that a single pulse represents one-half the period.
2. Scale the 3 and 1 pulse widths in proportion to the 2 pulse.
3. Set the amplitude of the pulses so that output amplitudes do not exceed values that would invalidate the assumed model structure using the current model estimate. For linear dynamical systems, this is a simple scaling operation.

The design procedure is similar for the 2-1-1 input:

1. Select the pulse width so that the frequencies of the 2 and 1 pulses bracket the frequency of the current estimate of the natural frequency for the dominant oscillatory mode. In the current work, the 2 and 1 pulses were determined as 4/3 and 2/3 times the pulse width corresponding to the current natural frequency estimate.
2. Set the amplitude of the pulses so that output amplitudes do not exceed values that would invalidate the assumed model structure using the current model estimate. For linear dynamical systems, this is a simple scaling operation.

Doublet inputs are sometimes designed to match the frequency of the current estimate of the natural frequency for the dominant oscillatory mode, but are also sometimes designed to have very thin pulse width to approximate a two-sided impulse, which theoretically contains all frequencies.

There are other input forms and input design methods[10], but square wave input forms have been shown to be simple and effective[9], so these input forms were selected for the flight test input design.

The test maneuver sequence begins with a simple unit amplitude doublet with a one second pulse width, which corresponds to a frequency of 0.5 Hz. After executing this initial maneuver, the data are analyzed in real time using equation error in the frequency domain, as described above. The requisite Fourier transforms for the parameter estimation in Eq. (17) are computed continuously in real time using Eqs. (21), (20), and (9). Based on the results from this analysis, a slightly more complex input, the 2-1-1, is designed and implemented. Input amplitudes and frequencies are calculated based on results from data produced by the previous doublet maneuver. Analysis of data from all preceding maneuvers (i.e., the doublet and 2-1-1) is used as the basis for designing amplitude and frequency for the slightly more complicated 3-2-1-1 input. Re-designs of the 3-2-1-1 input can continue based on the most recent data analysis until specific objectives (such as specified accuracy on any or all estimated parameters) are met. The sequential increase

in the input complexity is designed to correspond with the increasing accuracy of the model parameters as the maneuvers are executed. Total time for each maneuver includes 2-3 seconds of zero input before each test input to allow responses to settle to trim values in preparation for each maneuver. The delay is randomized uniformly on the interval [2,3] seconds to enrich the input spectrum. This delay also allows time for the data analysis and input design for the next maneuver.

Example

For longitudinal aircraft short period dynamics, the state vector **x**, input vector **u**, and output vector **y** in Eqs. (1) and (3) are defined by

$$\begin{aligned} \boldsymbol{x} &= \begin{bmatrix} \alpha & q \end{bmatrix}^T \quad \boldsymbol{u} = \begin{bmatrix} \delta_e \end{bmatrix} \\ \boldsymbol{y} &= \begin{bmatrix} \alpha & q & a_z \end{bmatrix}^T \end{aligned} \tag{23}$$

System matrices containing the model parameters are:

$$\boldsymbol{A} = \begin{bmatrix} Z_\alpha & Z'_q \\ M_\alpha & M_q \end{bmatrix} \qquad \boldsymbol{B} = \begin{bmatrix} Z_{\delta_e} \\ M_{\delta_e} \end{bmatrix} \tag{24}$$

$$\boldsymbol{C} = \begin{bmatrix} 1 & 0 \\ 0 & 1 \\ Z_\alpha \dfrac{V_o}{g} & Z_q \dfrac{V_o}{g} \end{bmatrix} \qquad \boldsymbol{D} = \begin{bmatrix} 0 \\ 0 \\ Z_{\delta_e} \dfrac{V_o}{g} \end{bmatrix} \tag{25}$$

The above model assumes $\dot{\alpha} \approx q$, so that $\dot{\alpha}$ effects can be subsumed into the Z'_q and M_q derivatives. Parameter Z'_q includes the inertial term, i.e., $Z'_q = 1 + Z_q$. The model also assumes a small trim angle of attack, so that $Z \approx -L$ and $a_z \approx a_{z_w}$.

In the first example, perturbation elevator inputs were applied to a known linear model to produce simulated state and output responses. The simulated aircraft is a conventional F-16[6] with forward c.g. position ($0.2\ \bar{c}$) in straight and level flight at 10,000 ft, trim angle of attack 7 deg, and Mach 0.37. The simulated states and outputs were corrupted with 20% gaussian random white noise. This made the signal-to-noise ratio 5-to-1 for each simulated state and output measurement. The elevator input was assumed to be measured without noise, which is a close approximation to reality. The true values of the model parameters used to generate the simulated test data are given in column 2 of Table 1. Parameter estimation was done using equation error in the frequency domain applied to the two state equations, as described above, with the Fourier transform computed recursively.

The initial doublet input is shown in Figure 3. Parameter estimation results based on simulated data from this input are given in column 3 of Table 1. In general, the parameter estimates are approximate, and the standard errors (in parentheses below each parameter estimate) are relatively large. Figure 4 is the 2-1-1 input design based on the results from the doublet maneuver data. The abscissa in Figure 4 shows that the 2-1-1 maneuver was executed after the doublet maneuver. Input amplitude was scaled to produce ±2.5 deg of α change from trim, which is typical for linear model validity. The input amplitude scaling was done by keeping track of the maximum absolute α deviation from trim during the doublet maneuver, α_{max} (in deg), then scaling the doublet input amplitude by the ratio $2.5/\alpha_{max}$. Pulse widths were designed according to the procedure outlined above. Parameter estimation results in column 4 of Table 1 show that the parameter estimates are approaching the true values with standard errors decreasing. A similar trend is shown in column 5 of Table 1, which contains results based on the data including the 3-2-1-1 maneuver shown in Figure 5. The 3-2-1-1 maneuver was designed based on analysis of data from the preceding doublet and 2-1-1 maneuvers. The abscissa in Figure 5 shows that the 3-2-1-1 maneuver was executed after the 2-1-1 maneuver.

Figure 6 shows the trend for the Z_α parameter with each identification cycle of maneuver design and data analysis. The estimated parameter values approach the true value with a decreasing standard error. Similar plots could be made for the other model parameters.

The technique was then applied to the full nonlinear F-16 simulation[6], with similar results. Figure 7 shows the elevator input design for a simulated flight test of the F-16 with forward c.g. position ($0.2\ \bar{c}$) in straight and level flight at 20,000 ft, trim angle of attack 20 deg, and Mach 0.27. Figure 8 shows the angle of attack and pitch rate response. The same output amplitude

constraint of ±2.5 deg in α was used and was successfully implemented via the input amplitude scaling.

Parameter estimation results for this case are given in Table 2 using the same format as Table 1. The "true" linear model parameter values shown in column 2 of Table 2 were obtained from the nonlinear simulation using central finite differences and 1% perturbations on the state and control variables. Performance of the algorithm was similar to that seen for the linear case at a lower trim angle of attack. Input amplitudes and pulse widths were adjusted adaptively and automatically to match the dynamics of the aircraft at this flight condition. Figure 9 shows the power spectrum of the input. The adaptive input design resulted in an input with a broad energy band centered at the "true" natural frequency, even though the algorithm had no information about the natural frequency of the system *a priori*.

The nonlinear simulation, the on-line maneuver design, and the on-line data analysis were all programmed in Matlab and ran on a Sun 200 MHz HyperSparc (serial processor, running SunOS 4.1.4) roughly twice as fast as real time.

Concluding Remarks

The approach to aircraft system identification proposed here changes the philosophy of aircraft dynamic modeling experimentation from designing test maneuvers based on *a priori* predictions of the dynamic characteristics and evaluating the data quality post-flight, to an in-flight adaptive approach that relies solely on measured flight data from the dynamical system to be modeled. The developed method implements the identification cycle of experiment design, parameter estimation, re-design of the experiment based on the estimation results, and so on repeatedly, until desired accuracy measures for the model parameters are met. Dynamic effects that are impossible to predict on the ground before the flight could be accounted for in real time by the automatic design of the test maneuvers in flight. *A priori* input design is avoided altogether. The procedure has reasonable computational requirements and could be implemented in flight in real time.

This work used simulation examples to demonstrate the in-flight system identification scheme. The method could be used for dimensional or non-dimensional parameter estimation, and could also be used with general nonlinear models, as long as the model is linear in the parameters. All states and inputs must be measured, but this should not be a problem in the flight test environment for which the method is intended. A more sophisticated algorithm would be required for multiple input maneuver design, but repeated applications of the present method to individual inputs, one at a time, might prove to be adequate.

The on-line data analysis in the frequency domain has the advantage of automatically removing trim values and measurement biases from the data because zero frequency is omitted from the Fourier transformation. In addition, the data is automatically filtered because only the specific frequencies corresponding to the dynamic motion of interest are included in the Fourier transformation.

Ultimately, the algorithm could be packaged as a subroutine to be included in flight control computer software. Since the algorithm is adaptive and requires no *a priori* analysis for the input design, it could be called on to execute appropriate test maneuvers for any flight condition throughout the flight envelope. This capability has obvious attraction for flight envelope expansion, flight control system design validation, aerodynamic parameter estimation, and simulator updates.

References

1. Gelb, A., et. al. *Applied Optimal Estimation*, The M.I.T. Press, Cambridge, MA. 1974.

2. Garcia-Velo, J. and Walker, B.K. "Aerodynamic Parameter Estimation for High-Performance Aircraft Using Extended Kalman Filtering," *Journal of Guidance, Control and Dynamics*, Vol. 20, No. 6, November-December 1997. pp. 1257-9.

3. Kokolios, A. "Use of a Kalman Filter for the Determination of Aircraft Aerodynamic Characteristics from Flight Test Data," AIAA Paper 94-0010, *32nd Aerospace Sciences Meeting & Exhibit*. Reno, NV. January 1994.

4. Bauer, J.E. and Andrisani, D. "Estimating Short-Period Dynamics using an Extended Kalman Filter," AIAA Paper AIAA-90-1277-CP, *Fifth Biannual Flight Test Conference*. Ontario, CA. May 1990.

5. Kaufman, H. "Aircraft Parameter Identification Using Kalman Filtering," *Proceedings of the National Electronics Conference*, Vol. XXV, pp. 85-9. December 1969.

6. Stevens, B.L. and Lewis, F.L. *Aircraft Control and Simulation*, John Wiley & Sons, Inc. New York, NY. 1992.

7. Morelli, E.A. "High Accuracy Evaluation of the Finite Fourier Transform Using Sampled Data", NASA TM 110340, June 1997.

8. Klein, V. "Aircraft Parameter Estimation in Frequency Domain", AIAA paper 78-1344, Atmospheric Flight Mechanics Conference, Palo Alto, CA, August 1978.

9. Morelli, E.A. "Flight Test Validation of Optimal Input Design and Comparison to Conventional Inputs," AIAA paper 97-3711, *AIAA Atmospheric Flight Mechanics Conference*. New Orleans, LA. August 1997.

10. Mehra, R.K. and Gupta, N.K. "Status of Input Design for Aircraft Parameter Identification," AGARD-CP-172, paper 12. May 1975.

Table 1 Linear Simulation Results, $\alpha_o = 7$ deg, $h_o = 10{,}000$ ft, $M_o = 0.37$

		Maneuver		
Parameter	True Value	Doublet	2-1-1	3-2-1-1
Z_α	–0.600	–0.791	–0.629	–0.599
		(0.054)	(0.030)	(0.022)
Z'_q	0.950	1.106	0.987	0.961
		(0.046)	(0.021)	(0.016)
Z_{δ_e}	–0.002	0.0010	–0.0015	–0.0016
		(0.0016)	(0.0008)	(0.0006)
M_α	–4.300	–3.598	–4.118	–4.193
		(0.137)	(0.094)	(0.043)
M_q	–1.200	–1.662	–1.178	–1.184
		(0.116)	(0.067)	(0.030)
M_{δ_e}	–0.090	–0.104	–0.088	–0.089
		(0.004)	(0.002)	(0.001)

Table 2 Nonlinear Simulation Results, $\alpha_o = 20$ deg, $h_o = 20{,}000$ ft, $M_o = 0.27$

		Maneuver		
Parameter	True Value	Doublet	2-1-1	3-2-1-1
Z_α	–0.260	–0.611	–0.266	–0.274
		(0.140)	(0.040)	(0.029)
Z'_q	0.954	1.103	0.886	0.911
		(0.101)	(0.036)	(0.028)
Z_{δ_e}	–0.0007	0.0023	–0.0014	–0.0009
		(0.0021)	(0.0009)	(0.0007)
M_α	–1.761	–1.613	–2.004	–1.878
		(0.108)	(0.039)	(0.033)
M_q	–0.611	–0.769	–0.591	–0.614
		(0.078)	(0.035)	(0.032)
M_{δ_e}	–0.0341	–0.0381	–0.0333	–0.0342
		(0.0016)	(0.0009)	(0.0008)

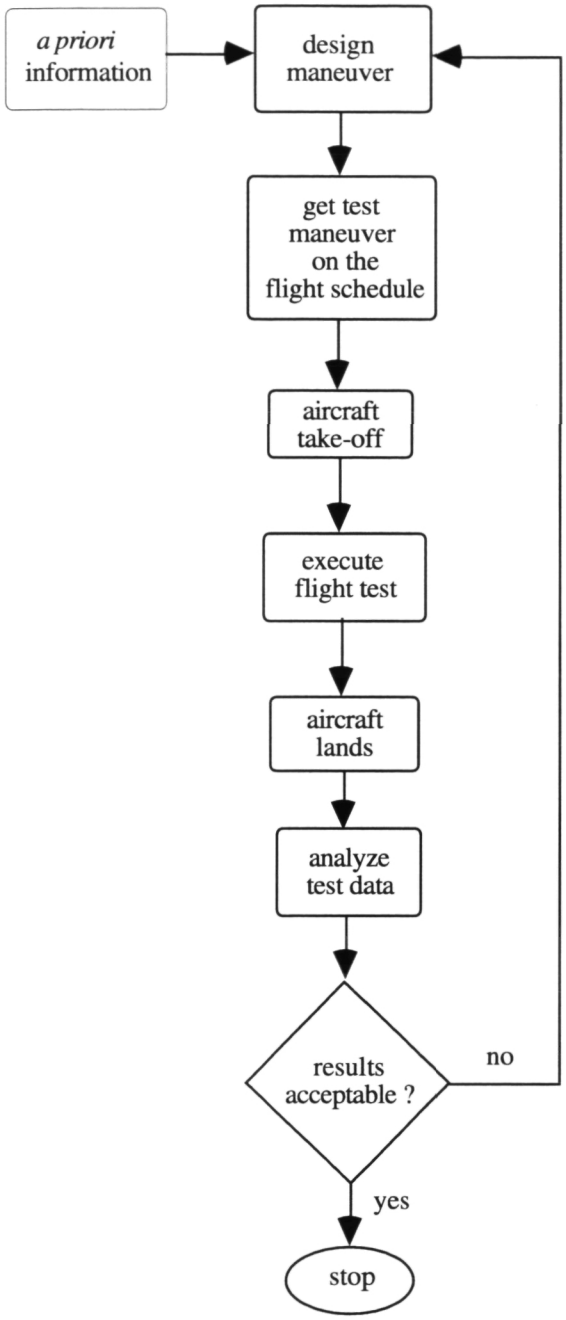

Figure 1 Conventional System Identification Cycle

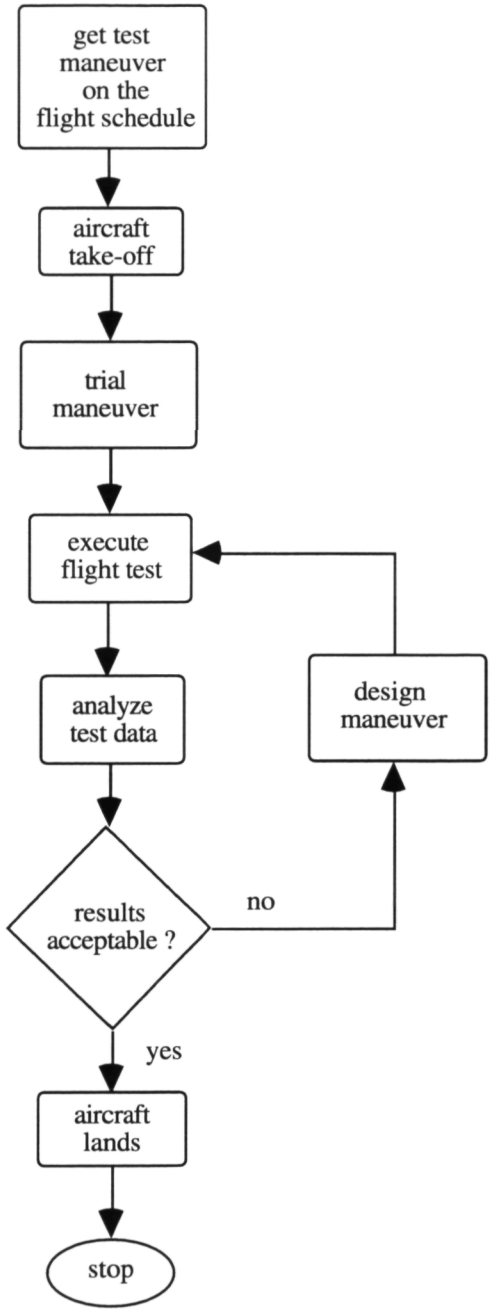

Figure 2 In-Flight System Identification

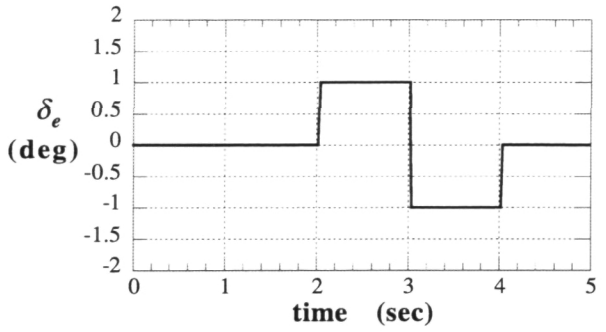

Figure 3 Doublet Input

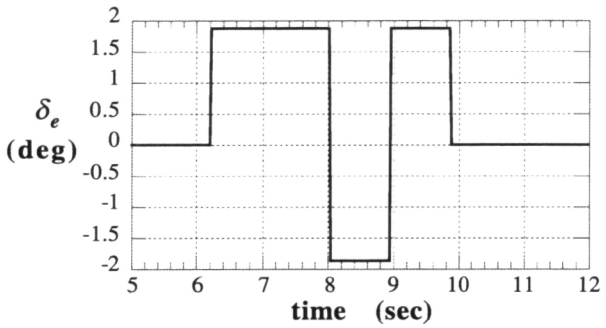

Figure 4 2-1-1 Input

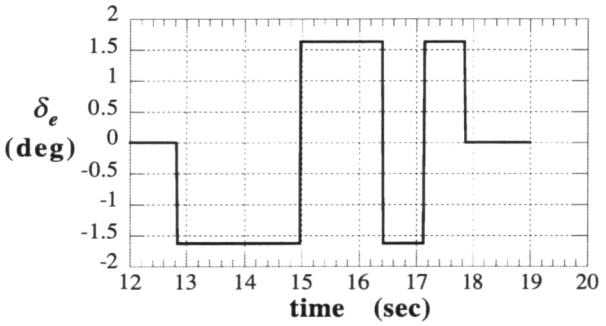

Figure 5 3-2-1-1 Input

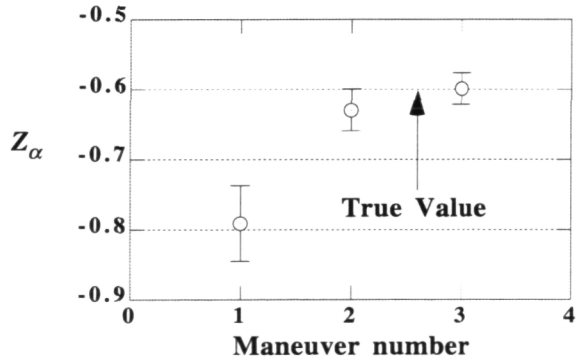

Figure 6 Z_α Parameter Estimation

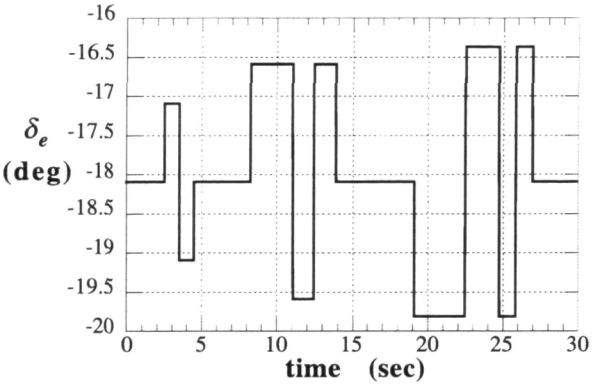

Figure 7 Nonlinear Simulation Input Sequence

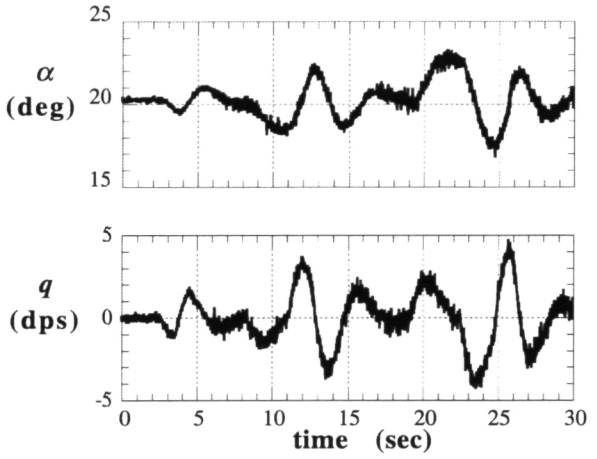

Figure 8 Nonlinear Simulation Response

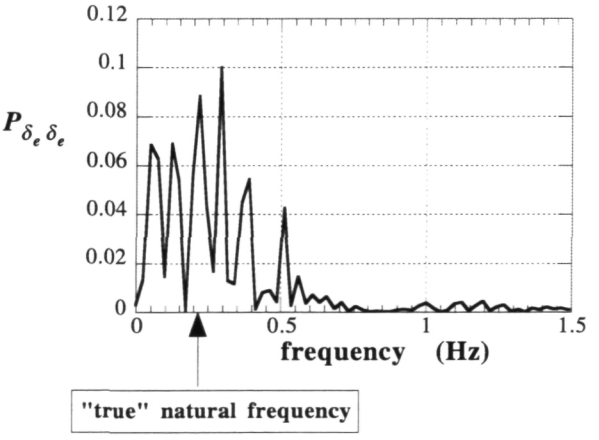

Figure 9 Input Power Spectrum